The Canadian Mineralogist
Vol. 38, pp. 163-173 (2000)

A NEW URANYL SHEET IN $K_5[(UO_2)_{10}O_8(OH)_9](H_2O)$: NEW INSIGHT INTO SHEET ANION-TOPOLOGIES

PETER C. BURNS[§] AND FRANCES C. HILL

Department of Civil Engineering and Geological Sciences, University of Notre Dame, 156 Fitzpatrick Hall, Notre Dame, Indiana 46556, U.S.A.

ABSTRACT

The structure of $K_5[(UO_2)_{10}O_8(OH)_9](H_2O)$, $Z = 4$, monoclinic, space group *Pn*, *a* 13.179(2), *b* 20.895(4), *c* 13.431(3) Å, β 106.316(3)°, has been solved and refined to $R = 7.8\%$ and a goodness-of-fit of 0.82 for 4349 unique observed ($F_o \geq 4\sigma_F$) reflections collected for a synthesized crystal using Mo*K*α X-radiation and a CCD detector. The structure is dominated by previously unknown sheets of edge- and vertex-sharing uranyl polyhedra parallel to (100), with K cations and H_2O groups in the interlayer. The sheets contain 20 symmetrically distinct U^{6+} cations, each of which is associated with an approximately linear $(UO_2)^{2+}$ uranyl ion (*Ur*), and is coordinated by four or five additional anions at the equatorial positions of square (2 polyhedra) and pentagonal (18 polyhedra) bipyramids, respectively. As is the case with other sheets of uranyl polyhedra, the anion topology of the sheet can be generated using a chain-stacking sequence; however, the sequence is unique and for the first time involves the occurrence of **P** chains flanked by **U** or **D** chains of opposite directional sense. This example serves to further demonstrate the structural complexity that is possible in sheets of uranyl polyhedra.

Keywords: uranium, uranyl oxide hydrate of potassium, synthetic, anion topology, crystal structure.

SOMMAIRE

Nous avons determiné et affiné la structure du composé $K_5[(UO_2)_{10}O_8(OH)_9](H_2O)$, $Z = 4$, monoclinique, groupe spatial *Pn*, *a* 13.179(2), *b* 20.895(4), *c* 13.431(3) Å, β 106.316(3)°, jusqu'à un résidu *R* de 7.8% et une concordance de 0.82 en utilisant 4349 réflexions uniques observées ($F_o \geq 4\sigma_F$) et prélevées sur cristal synthétique avec rayonnement Mo*K*α et un détecteur de type CCD. La structure contient comme élément dominant des feuillets parallèles à (100), de géométrie jusque là inconnue, faits de polyèdres à uranyle partageant des arêtes et des coins, avec des cations K et des groupes H_2O dans les interfeuillets. Ces feuillets contiennent vingt cations U^{6+} symétriquement distincts; chacun de ceux-ci est associé à l'ion $(UO_2)^{2+}$ (uranyle, *Ur*), à peu près linéaire, en coordinence avec quatre ou cinq anions additionnels aux positions équatoriales d'un agencement carré (deux polyèdres) et pentagonal (18 polyèdres), respectivement, et bipyramidal. Tout comme dans les autres feuillets contenant des polyèdres à uranyle, on peut expliquer la topologie des anions du feuillet par propagation d'un empilement de chaînes; la séquence observée est unique, et implique pour la première fois des chaînes **P**, que longent des chaînes allant dans le sens opposé, soit vers le haut (**U**) ou vers le bas (**D**). Ce schéma sert à démontrer la complexité structurale possible dans les feuillets contenant des polyèdres à uranyle.

(Traduit par la Rédaction)

Mots-clés: uranium, oxyde d'uranyle hydraté de potassium, synthèse, topologie des anions, structure cristalline.

INTRODUCTION

There are ~200 uranyl minerals (Mandarino 1999) that are important for understanding the genesis of U deposits (Frondel 1958, Finch & Ewing 1992). Uranyl minerals are significant in several areas of environmental concern. They are present in the mill tailings that result from the mining of U, and are precipitated in soils that are contaminated with actinide elements. They will be the dominant products of alteration of spent nuclear fuel in a geological repository if the conditions are oxidizing and the fuel comes in contact with water, such as is likely to occur at the proposed repository at Yucca Mountain, Nevada (Finn *et al.* 1996, Wronkiewicz *et al.* 1996). An understanding of the complex crystal chemistry of these minerals is essential to the prediction of their impact on the release of radionuclides from nuclear waste under repository conditions.

§ *E-mail address*: pburns@nd.edu

The paragenesis of uranyl minerals should be related to the energetics and stabilities of the underlying crystal structures. However, the links will only be revealed following a substantial improvement of our knowledge of the crystal chemistry of uranyl minerals, which lags well behind that of many other mineral groups (despite their obvious importance). The structures have been determined and refined for only ~60 uranyl minerals, less than one-third of the known species. This is due to severe experimental difficulties; uranyl minerals are extreme absorbers of X-rays, many do not form crystals of a size suitable for structure analysis using conventional techniques, and others dehydrate, causing deterioration of the crystals. The recent introduction of CCD-based X-ray detectors to mineralogical studies (Burns 1998a) has resulted in significant advances in our understanding of the structures of uranyl minerals (Burns 1997, 1998b, c, d, 1999a, 2000a, b, Burns & Finch 1999, Burns & Hanchar 1999, Hill & Burns 1999, Burns & Hill 2000). Surprising discoveries include the presence of U^{5+} in wyartite (Burns & Finch 1999), uranyl phosphate chains in parsonsite (Burns 2000b), and extraordinarily complex sheets of uranyl polyhedra in vandendriesscheite (Burns 1997) and wölsendorfite (Burns 1999a). Following the discovery of the wölsendorfite sheet with a primitive repeat of 56 Å, Burns (1999a) noted that such complex sheets contain components of two or more simpler sheets observed in other minerals, suggesting that many new sheets of uranyl polyhedra may await discovery. A substantial portion of the structural energetics of uranyl minerals must depend upon the connectivity of the sheets of polyhedra. The details of the sheet anion-topologies may therefore be a key to understanding and predicting the thermodynamics of these phases.

We have undertaken studies of synthetic (<200°C) uranyl phases to obtain new insight into the structures, stabilities, and chemistries of uranyl minerals. Crystals of a K uranyl oxide hydrate (hereafter designated *KUOH*) that contains a new sheet of uranyl polyhedra have been obtained, and the details of the structure are presented herein.

Experimental Methods

Synthesis of crystals

Amber-yellow crystals of *KUOH* were obtained from synthesis experiments intended to give boltwoodite, modified from the methods of Vochten *et al.* (1997). A solution containing 0.01M uranium oxynitrate (Alfa Æsar), $UO_2(NO_3)_2$•$6H_2O$, and 0.1M KCl (Fisher Scientific) was prepared using ultrapure water. The pH was adjusted to ~12 using 5M KOH (Fisher Scientific). One gram of natural quartz crystals was added to the solution in a Teflon-lined Parr bomb. The reactants were held at 225°C for 72 h, and the products were allowed to cool slowly. The resulting crystals were separated from the solution by filtration and were washed three times using ultrapure water. The crystals consisted of ~95% boltwoodite and ~5% of *KUOH*.

X-ray diffraction

An acicular crystal with sharp extinction and uniform optical properties was selected for the X-ray study. The crystal was mounted on a Bruker PLATFORM 3-circle goniometer equipped with a 1K SMART CCD (charge-coupled device) detector and a crystal-to-detector distance of 5 cm (Burns 1998a).

More than 75% of a sphere of data was collected to ~57° 2θ using monochromatic Mo*K*α X-radiation and frame widths of 0.3° in ω, with 180 s used to acquire each frame. The final unit-cell dimensions (Table 1) were refined on the basis of 2785 reflections using least-squares techniques. Data were collected in approximately 95 hours; comparison of the intensities of equivalent reflections collected at different times during the data collection showed no evidence of significant decay. The three-dimensional data were reduced and corrected for Lorentz, polarization, and background effects using the Bruker program SAINT. An empirical absorption-correction was done using the program SADABS (G. Sheldrick, unpubl. computer program) on the basis of the intensities of equivalent reflections. A total of 32,837 reflections was collected; the merging of equivalent reflections gave 16,067 unique reflections, with 4349 classed as observed ($F_o \geq 4\sigma_F$).

Structure Solution and Refinement

Scattering curves for neutral atoms, together with anomalous dispersion corrections, were taken from *International Tables for X-Ray Crystallography, Vol. IV* (Ibers & Hamilton 1974). The Bruker SHELXTL Version 5 system of programs was used for the refinement of the crystal structure.

Reflection statistics and systematic absences indicated space groups *Pn* or *P*2/*n*. Attempts to solve the structure in the centrosymmetyric space group failed, and space group *Pn* was verified by the successful solu-

TABLE 1. MISCELLANEOUS INFORMATION PERTAINING TO THE STRUCTURE REFINEMENT OF *KUOH*

a (Å)	13.179(2)	Crystal size (μm)	80 x 10 x 5
b (Å)	20.895(4)		
c (Å)	13.431(3)	Total ref.	32,837
β (°)	106.316(3)	Unique ref.	16,067
V (Å^3)	3549.5(9)	Unique $\|F_o\| \geq 4\sigma_F$	4349
Space group	*Pn*	Final R (%)	7.8
F(000)	5320	S	0.82
μ (mm^{-1})	46.1		
D_{calc} (g/cm^3)	5.979		

Unit-cell contents: $4\{K_2[(UO_2)_{10}O_8(OH)_9](H_2O)\}$

$R = \Sigma(|F_o|-|F_c|)/\Sigma|F_o|$

$S = [\Sigma w(|F_o|-|F_c|)^2/(m-n)]^{½}$, for m observations and n parameters

tion of the structure by direct methods. The initial model included the positions of the U atoms, with K cations and anions located in difference-Fourier maps after least-squares refinement of the model. The final model involved refinement of the atomic positional parameters, isotropic-displacement parameters, and a weighting scheme for the structure factors. Refinement of this very large structure was difficult owing to weak data and pseudosymmetry. Some of the uranyl ion U^{6+}–O bond-lengths refined to values outside the range in well-refined structures; the "soft" constraint that these bond lengths be ~1.8 Å was imposed during the final cycles of refinement, and did not change the agreement index (R). Two overall displacement parameters were refined for the anions, one corresponding to O and the other to OH and H_2O groups. Refinement of anisotropic-displacement parameters for the cations only reduced R by ~0.5%, and led to instability of the refinement. The final R was 7.8% for the isotropic model for 4349 unique observed ($F_o \geq 4\sigma_F$) reflections, and the goodness-of-fit (S) was 0.82. The final atom parameters are given in Table 2, and selected mean interatomic distances and angles are given in Table 3. Calculated and observed structure-factors are available from the Depository of Unpublished Data, CISTI, National Research Council, Ottawa, Ontario K1A 0S2, Canada.

TABLE 2. ATOM PARAMETERS FOR *KUOH*

	x	y	z	$*U_{eq}$
U(1)	0.0199(4)	0.1582(3)	0.4374(4)	101(12)
U(2)	0.0381(4)	0.3497(3)	0.4560(4)	96(11)
U(3)	0.0171(3)	-0.2499(2)	0.4503(4)	69(10)
U(4)	0.0321(4)	-0.0584(2)	0.4410(4)	121(12)
U(5)	0.0161(4)	0.0496(3)	0.1564(4)	108(12)
U(6)	0.0149(4)	0.5472(2)	0.4491(4)	112(11)
U(7)	-0.0792(4)	-0.0585(2)	-0.0899(4)	40(10)
U(8)	-0.0691(4)	0.1618(2)	-0.0814(4)	96(12)
U(9)	-0.0595(3)	-0.2485(2)	-0.0687(3)	58(9)
U(10)	-0.0594(3)	0.5488(2)	-0.0669(3)	82(8)
U(11)	-0.0578(4)	0.0484(3)	0.6329(4)	72(11)
U(12)	-0.0449(3)	0.3508(2)	-0.0686(4)	51(10)
U(13)	0.0336(4)	-0.3528(2)	0.1738(4)	162(12)
U(14)	0.0453(3)	0.2366(2)	0.1732(3)	83(10)
U(15)	0.0422(3)	0.4578(2)	0.1754(4)	101(11)
U(16)	0.0273(4)	-0.1391(2)	0.1651(4)	155(12)
U(17)	-0.0724(3)	-0.3514(2)	0.6390(3)	61(10)
U(18)	-0.5553(4)	-0.2376(2)	0.1496(3)	122(12)
U(19)	-0.0474(4)	-0.1458(2)	-0.3560(4)	96(11)
U(20)	-0.0539(4)	0.4562(2)	-0.3467(4)	110(12)
K(1)	0.263(2)	-0.352(2)	0.656(2)	288(71)
K(2)	0.255(2)	0.053(1)	-0.362(2)	150(54)
K(3)	0.211(1)	0.048(1)	-0.075(2)	34(39)
K(4)	0.211(2)	0.653(1)	-0.069(2)	119(47)
K(5)	0.265(2)	0.244(1)	0.654(2)	194(60)
K(6)	0.210(2)	0.240(1)	-0.038(2)	272(70)
K(7)	-0.291(2)	-0.457(1)	0.454(2)	260(70)
K(8)	0.262(2)	-0.162(1)	0.625(2)	161(56)
K(9)	-0.299(2)	0.148(1)	0.455(2)	265(68)
K(10)	0.268(2)	0.455(2)	0.641(3)	318(78)
O(1)	0.146(3)	0.152(3)	0.534(3)	101(11)
O(2)	-0.113(3)	0.160(3)	0.347(4)	101(11)
O(3)	0.175(2)	0.348(3)	0.529(4)	101(11)
O(4)	-0.102(2)	0.352(3)	0.380(4)	101(11)
O(5)	-0.113(3)	-0.237(3)	0.360(4)	101(11)
O(6)	0.151(3)	-0.265(3)	0.533(4)	101(11)
O(7)	-0.100(3)	-0.072(2)	0.364(4)	101(11)
O(8)	0.169(2)	-0.059(2)	0.516(4)	101(11)
O(9)	-0.111(3)	0.056(3)	0.179(4)	101(11)
O(10)	0.145(2)	0.040(2)	0.137(4)	101(11)
O(11)	-0.107(3)	0.525(2)	0.356(4)	101(11)
O(12)	0.150(3)	0.556(3)	0.532(4)	101(11)
O(13)	0.055(3)	-0.048(3)	-0.093(5)	101(11)
O(14)	-0.218(2)	-0.069(2)	-0.097(4)	101(11)
O(15)	0.066(2)	0.160(3)	-0.087(5)	101(11)
O(16)	-0.203(2)	0.182(2)	-0.079(5)	101(11)
O(17)	-0.186(3)	-0.238(2)	-0.047(4)	101(11)
O(18)	0.067(3)	-0.255(3)	-0.096(6)	101(11)
O(19)	0.072(3)	0.562(3)	-0.081(5)	101(11)
O(20)	-0.202(2)	0.531(2)	-0.096(4)	101(11)
O(21)	-0.184(3)	0.043(3)	0.539(3)	101(11)
O(22)	0.071(3)	0.044(3)	0.727(4)	101(11)
O(23)	-0.160(3)	0.349(2)	-0.029(4)	101(11)
O(24)	0.068(3)	0.348(3)	-0.121(4)	101(11)

TABLE 2 (continued). ATOM PARAMETERS FOR *KUOH*

	x	y	z	$*U_{eq}$
O(25)	0.169(2)	-0.358(2)	0.167(4)	101(11)
O(26)	-0.097(3)	-0.345(3)	0.194(5)	101(11)
O(27)	0.175(3)	0.217(2)	0.163(5)	101(11)
O(28)	-0.088(3)	0.261(3)	0.167(5)	101(11)
O(29)	-0.084(3)	0.433(2)	0.186(5)	101(11)
O(30)	0.180(2)	0.464(2)	0.174(4)	101(11)
O(31)	-0.104(3)	-0.159(3)	0.171(5)	101(11)
O(32)	0.164(2)	-0.145(2)	0.157(4)	101(11)
O(33)	-0.213(2)	-0.345(3)	0.573(5)	101(11)
O(34)	0.064(2)	-0.352(3)	0.724(4)	101(11)
O(35)	-0.421(3)	-0.238(3)	0.236(4)	101(11)
O(36)	-0.692(2)	-0.259(2)	0.086(4)	101(11)
O(37)	0.082(3)	-0.152(3)	-0.261(4)	101(11)
O(38)	-0.184(3)	-0.136(3)	-0.440(5)	101(11)
O(39)	0.073(3)	0.474(2)	-0.255(4)	101(11)
O(40)	-0.190(2)	0.446(3)	-0.431(4)	101(11)
O(41)	-0.015(5)	0.450(3)	-0.002(5)	101(11)
O(42)	-0.024(5)	0.151(4)	0.092(6)	101(11)
O(43)	-0.011(5)	-0.152(4)	-0.009(6)	101(11)
O(44)	-0.032(4)	-0.047(4)	0.079(4)	101(11)
O(45)	-0.028(4)	-0.055(3)	-0.414(4)	101(11)
O(46)	-0.010(5)	0.253(3)	-0.004(5)	101(11)
O(47)	0.023(5)	-0.149(3)	0.506(5)	101(11)
O(48)	0.034(4)	0.450(3)	0.531(4)	101(11)
O(49)	-0.015(5)	0.551(4)	0.105(5)	101(11)
O(50)	-0.032(4)	-0.353(3)	0.483(4)	101(11)
O(51)	-0.064(4)	0.550(3)	0.564(4)	101(11)
O(52)	-0.060(5)	-0.249(3)	0.587(5)	101(11)
O(53)	0.023(4)	-0.247(2)	0.117(4)	101(11)
O(54)	-0.507(5)	-0.255(2)	0.014(5)	101(11)
O(55)	-0.026(4)	-0.340(2)	-0.013(4)	101(11)
O(56)	-0.047(4)	0.144(3)	0.578(5)	101(11)
OH(57)	0.095(4)	-0.161(3)	0.339(5)	100(20)
OH(58)	-0.112(4)	0.052(3)	-0.048(4)	100(20)
OH(59)	0.064(4)	0.349(2)	0.126(5)	100(20)
OH(60)	-0.007(4)	0.346(2)	-0.364(4)	100(20)
OH(61)	-0.104(4)	0.551(3)	-0.256(4)	100(20)
OH(62)	-0.117(5)	-0.163(2)	-0.216(5)	100(20)
OH(63)	0.001(4)	0.053(3)	0.472(4)	100(20)
OH(64)	0.104(4)	0.262(2)	0.349(5)	100(20)
OH(65)	0.092(5)	0.131(3)	0.294(5)	100(20)
OH(66)	0.089(4)	0.555(3)	0.299(4)	100(20)
OH(67)	0.093(4)	-0.306(2)	0.322(4)	100(20)
OH(68)	0.080(4)	-0.019(2)	0.284(4)	100(20)
OH(69)	0.107(4)	0.413(2)	0.338(4)	100(20)
OH(70)	-0.127(4)	-0.307(2)	0.762(4)	100(20)
OH(71)	-0.112(4)	0.135(2)	-0.259(4)	100(20)
OH(72)	-0.121(4)	-0.021(2)	0.734(4)	100(20)
OH(73)	-0.129(5)	0.421(2)	-0.217(5)	100(20)
OH(74)	-0.617(5)	-0.264(3)	0.303(5)	100(20)
H_2O(75)	0.229(3)	-0.043(2)	-0.209(3)	100(20)
H_2O(76)	0.221(4)	0.350(4)	-0.216(4)	100(20)

$*U_{eq} = U_{eq}$ Å^2 x 10^4

TABLE 3. SELECTED MEAN INTERATOMIC DISTANCES (Å) AND ANGLES (°) IN THE STRUCTURE OF *KUOH*

<U(1)-O_{Ur}>	1.81	<U(11)-O_{Ur}>	1.79
<U(1)-$O_2(OH)_3$>	2.44	<U(11)-$O_2(OH)_3$>	2.36
<O_{Ur}-U(1)-O_{Ur}>	175(3)	<O_{Ur}-U(11)-O_{Ur}>	173(2)
<U(2)-O_{Ur}>	1.82	<U(12)-O_{Ur}>	1.78
<U(2)-$O_2(OH)_3$>	2.46	<U(12)-$O_2(OH)_3$>	2.40
<O_{Ur}-U(2)-O_{Ur}>	179(3)	<O_{Ur}-U(12)-O_{Ur}>	174(2)
<U(3)-O_{Ur}>	1.83	<U(13)-O_{Ur}>	1.82
<U(3)-$O_3(OH)_2$>	2.43	<U(13)-$O_3(OH)_2$>	2.33
<O_{Ur}-U(3)-O_{Ur}>	176(3)	<O_{Ur}-U(13)-O_{Ur}>	174(3)
<U(4)-O_{Ur}>	1.79	<U(14)-O_{Ur}>	1.81
<U(4)-$O_2(OH)_3$>	2.42	<U(14)-$O_2(OH)_3$>	2.39
<O_{Ur}-U(4)-O_{Ur}>	170(2)	<O_{Ur}-U(14)-O_{Ur}>	173(3)
<U(5)-O_{Ur}>	1.79	<U(15)-O_{Ur}>	1.80
<U(5)-$O_2(OH)_3$>	2.42	<U(15)-$O_2(OH)_3$>	2.36
<O_{Ur}-U(5)-O_{Ur}>	177(2)	<O_{Ur}-U(15)-O_{Ur}>	167(2)
<U(6)-O_{Ur}>	1.81	<U(16)-O_{Ur}>	1.82
<U(6)-$O_2(OH)_1$>	2.28	<U(16)-$O_2(OH)_2$>	2.42
<O_{Ur}-U(6)-O_{Ur}>	168(3)	<O_{Ur}-U(16)-O_{Ur}>	163(2)
<U(7)-O_{Ur}>	1.80	<U(17)-O_{Ur}>	1.83
<U(7)-$O_3(OH)_2$>	2.41	<U(17)-$O_3(OH)_2$>	2.33
<O_{Ur}-U(7)-O_{Ur}>	176(3)	<O_{Ur}-U(17)-O_{Ur}>	171(2)
<U(8)-O_{Ur}>	1.81	<U(18)-O_{Ur}>	1.82
<U(8)-$O_2(OH)_3$>	2.37	<U(18)-$O_2(OH)_3$>	2.37
<O_{Ur}-U(8)-O_{Ur}>	168(2)	<O_{Ur}-U(18)-O_{Ur}>	162(3)
<U(9)-O_{Ur}>	1.79	<U(19)-O_{Ur}>	1.84
<U(9)-$O_3(OH)_2$>	2.36	<U(19)-$O_3(OH)_2$>	2.43
<O_{Ur}-U(9)-O_{Ur}>	176(3)	<O_{Ur}-U(19)-O_{Ur}>	173(3)
<U(10)-O_{Ur}>	1.83	<U(20)-O_{Ur}>	1.84
<U(10)-$O_3(OH)_1$>	2.34	<U(20)-$O_2(OH)_3$>	2.36
<O_{Ur}-U(10)-O_{Ur}>	162(3)	<O_{Ur}-U(20)-O_{Ur}>	173(3)

Description of the Structure

Projection of the structure along [100] (Fig. 1) reveals the presence of sheets of uranyl polyhedra parallel to (100), with K cations and H_2O groups located in the interlayer. This is in accord with other uranyl oxide hydrate structures, each of which contain sheets of polyhedra of higher bond-valence, with lower-valence cations and H_2O groups located in interlayer positions. This structural theme also dominates other groups of uranyl structures, including uranyl silicates, phosphates, vanadates, arsenates, and molybdates (Burns *et al.* 1996).

Formula of KUOH

All atoms in the structure are on general positions in the space group *Pn* (Table 2). Bond-valence sums calculated using parameters for U–O bonds (Burns *et al.* 1997b) and K–O bonds (Brese & O'Keeffe 1991) permitted the distinction of O, $(OH)^-$ and H_2O. The formula of the crystal studied is therefore $K_5[(UO_2)_{10}O_8(OH)_9](H_2O)$, $Z = 4$.

Cation polyhedra

Twenty symmetrically distinct U^{6+} cations occur in the structure. Each is strongly bonded to two O atoms, resulting in approximately linear $(UO_2)^{2+}$ uranyl ions (*Ur*), as is almost invariably the case in uranyl phases (Burns *et al.* 1997b). The mean U–O_{Ur} bond lengths are all ~1.8 Å, as required by the constraints imposed on the refinement, with O_{Ur}–U–O_{Ur} bond angles ranging between 162(2) and 179(3)°. Eighteen of the uranyl ions

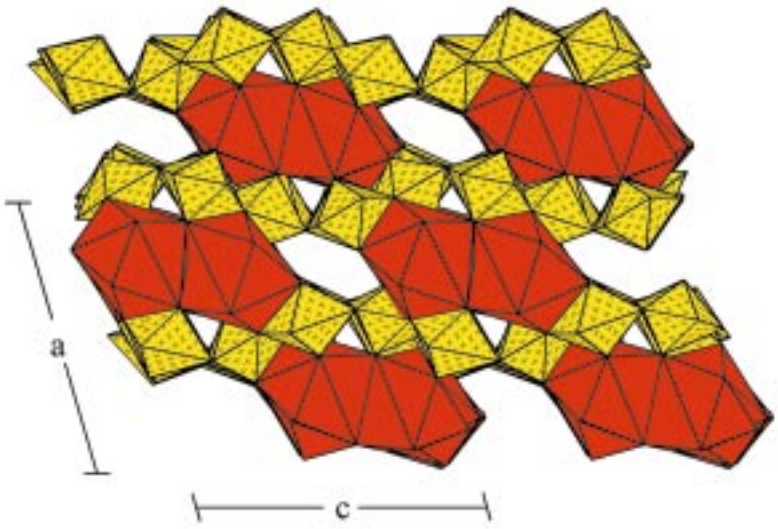

FIG. 1. Polyhedral representation of the structure of *KUOH* projected along [010]. *Ur*ϕ_n polyhedra: yellow, Kϕ_n polyhedra: orange.

are coordinated by five anions arranged at the equatorial vertices of pentagonal bipyramids capped with the O_{Ur} atoms. The pentagonal bipyramid is the most common U^{6+} coordination polyhedron in uranyl minerals (Evans 1963, Burns *et al.* 1997b). The mean $U–O_{eq}$ (*eq*: equatorial) bond lengths range from 2.33 to 2.44 Å, in accord with the mean value of 2.37(9) Å for $U–O_{eq}$ bonds in many $Ur\phi_5$ polyhedra in well-refined structures (Burns *et al.* 1997b). The equatorial anions of twelve of these polyhedra are comprised of two O atoms and three $(OH)^-$ groups, whereas the other six contain three O atoms and two $(OH)^-$ groups. Two uranyl ions, U(6) and U(10), are coordinated by four anions arranged at the vertices of strongly distorted square bipyramids capped by the O_{Ur} atoms. This U^{6+} polyhedron is common in uranyl phosphates and arsenates that contain sheets based upon the autunite anion-topology (Burns *et al.* 1996), but is not common in sheets together with uranyl pentagonal bipyramids. Exceptions are curite (Taylor *et al.* 1981), its synthetic Sr analog (Burns & Hill 2000), and sayrite (Piret *et al.* 1983). The $Ur\phi_4$ polyhedra in *KUOH* are strongly distorted (Fig. 2), and are similar to the polyhedra in the curite sheet (Taylor *et al.* 1981, Burns & Hill 2000). The equatorial anions in each correspond to three O and one $(OH)^-$, with the mean $U–O_{eq}$ bond lengths being 2.28 and 2.34 Å, in agreement with the mean $U–O_{eq}$ bond length of 2.28(5) in numerous $Ur\phi_4$ polyhedra in well-refined structures (Burns *et al.* 1996).

The structure contains ten symmetrically distinct K cations, each of which is located in the interlayer. Several of the $K\phi_n$ polyhedra are surrounded by ligands at distances in the range 3.0 to 3.4 Å, making description of the coordination polyhedra somewhat subjective. All K cations are coordinated by at least six ligands with bond lengths less than 3.1 Å, and some have as many as ten ligands within 3.4 Å. Coordinating ligands correspond to O_{Ur} anions, O and $(OH)^-$ anions located at the equatorial positions of uranyl polyhedra within the sheets, and H_2O groups in the interlayer. The $K\phi_n$ polyhedra share edges and faces, forming double-wide chains that are parallel to [010] (Fig. 3).

Sheets of uranyl polyhedra

Uranyl polyhedra polymerize by edge- and vertex-sharing, forming complex sheets parallel to (100) (Fig. 2), with the uranyl ions oriented roughly perpendicular to the plane of the sheet. The sheet, with a primitive repeat-distance of 20.9 Å, is more complex than

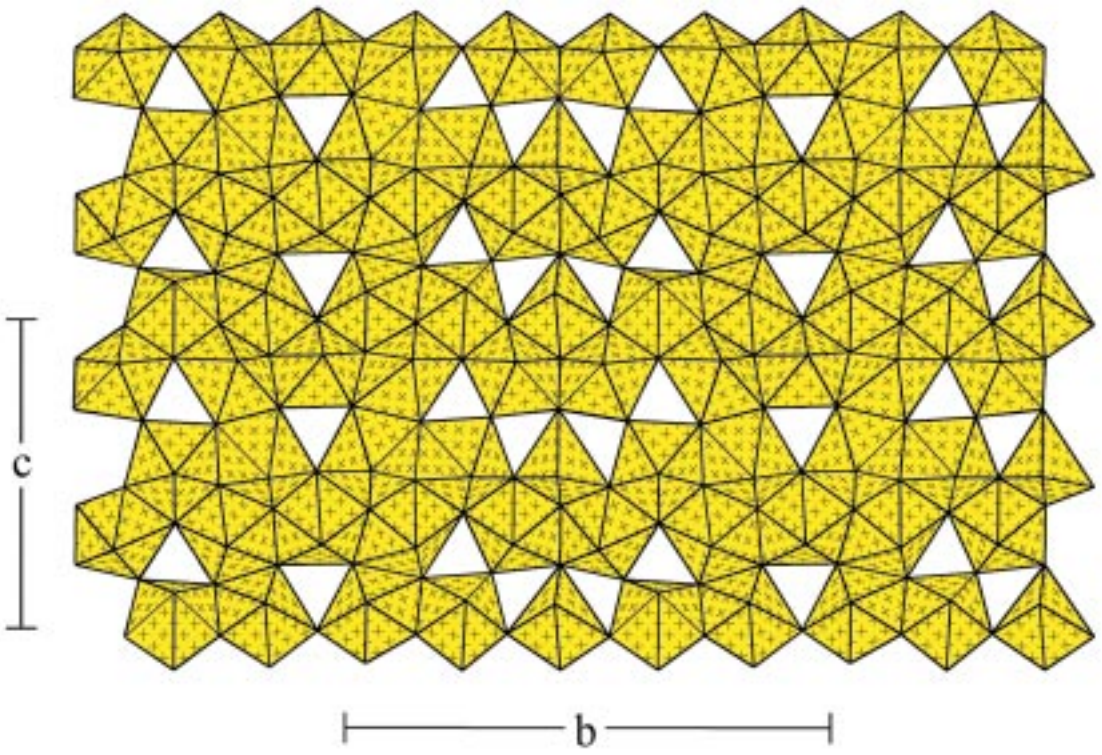

FIG. 2. Polyhedral representation of the sheet of uranyl polyhedra in the structure of *KUOH* projected onto (100).

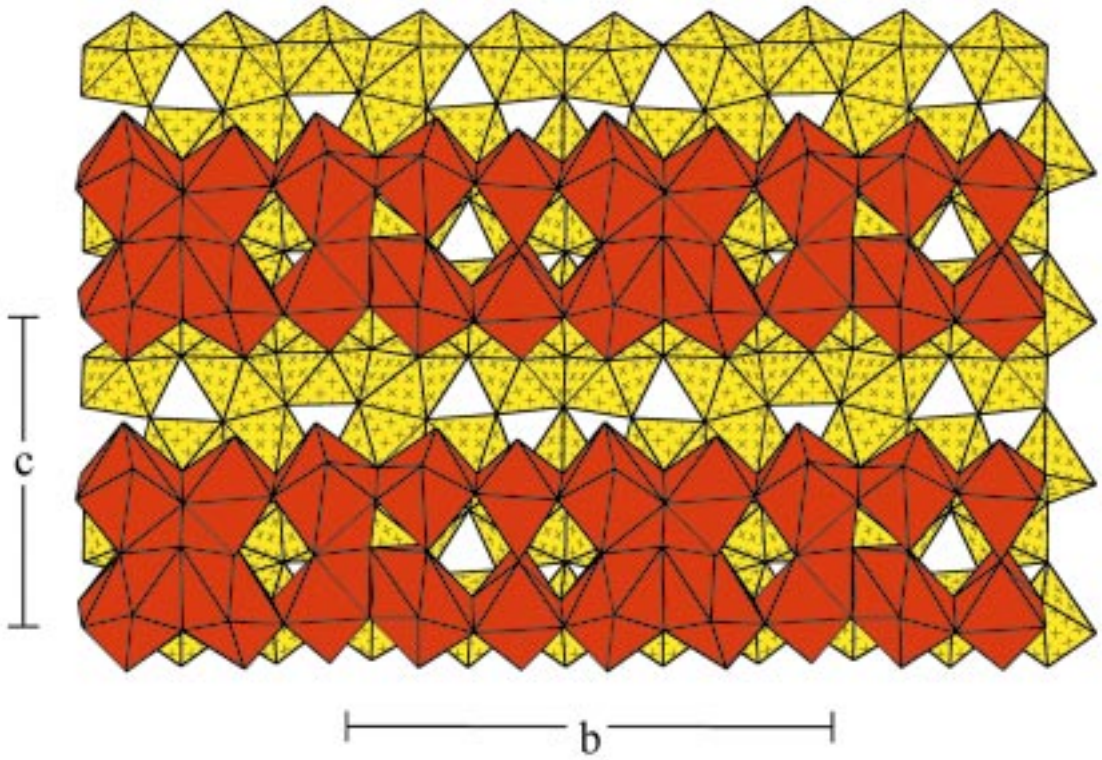

FIG. 3. Polyhedral representation of the interlayer in the structure of *KUOH* projected onto (100). *Ur*ϕ_n polyhedra: yellow, Kϕ_n polyhedra: orange.

most sheets of uranyl polyhedra, except for the vandendriesscheite sheet (41.4 Å) and the wölsendorfite sheet (56.0 Å). The sheet is topologically unique amongst minerals and synthetic uranyl phases; thus it provides additional insights into the complex connectivities of such sheets.

SHEET ANION-TOPOLOGIES IN URANYL OXIDE HYDRATES

The sheet anion-topology approach for comparing sheets of uranyl polyhedra and other polyhedra of higher bond-valence was introduced by Burns *et al.* (1996). It is not unusual for substantially different sheets to correspond to the same underlying topological arrangement of anions. Miller *et al.* (1996) developed the sheet anion-topology approach for uranyl oxide hydrates, and introduced representations of the topologies as chain-stacking sequences. With the exception of the curite anion-topology, only four chains of polygons are required to construct each of the anion topologies that correspond to sheets that contain only uranyl polyhedra (square, pentagonal, or hexagonal bipyramids); these are shown in Figure 4a. The **P** chain is composed of edge-sharing pentagons, the **R** chain contains rhombs, and the **H** chain contains edge-sharing hexagons. The arrowhead chains (**U** and **D**), which have a directional aspect, contain both pentagons and triangles, arranged such that each triangle shares an edge with a pentagon, and the opposite corner with another pentagon in the chain.

Generation of anion topologies using chain-stacking sequences is an efficient way of understanding the relationships among the complex sheets recently found in several minerals. This approach may be a key to understanding the links between complex structures, such as those of vandendriesscheite and wölsendorfite, and mineral paragenesis. Here we provide an overview of the different anion-topologies and corresponding chain-stacking sequences for sheets in uranyl oxide hydrate minerals and synthetic compounds, and restrict our discussion to sheets that contain only uranyl polyhedra. Burns (1999d) extended this approach to various sheets that contain other cation polyhedra of higher bond-valence in addition to uranyl.

Protasite (α–U_3O_8) *anion-topology*

The protasite anion-topology (Fig. 5a) is the basis of sheets that occur in protasite, becquerelite, billietite (Pagoaga *et al.* 1987), richetite (Burns 1998b), com-

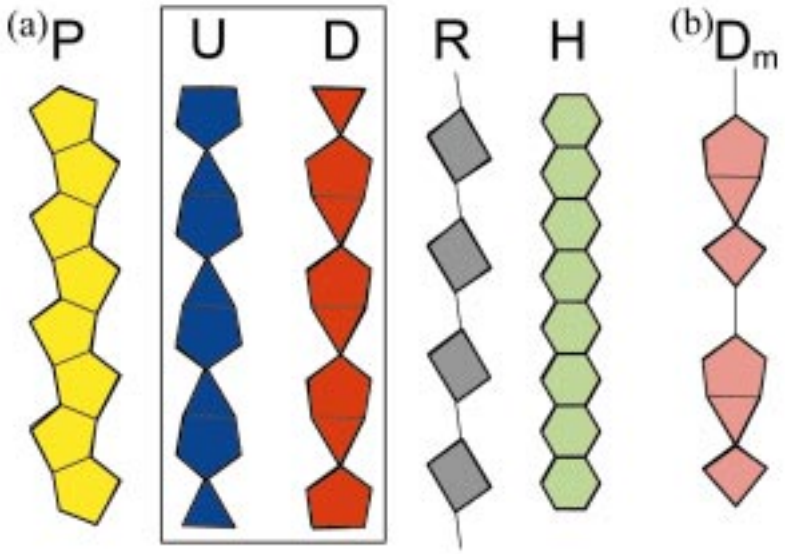

FIG. 4. Chains used to represent anion topologies as chain-stacking sequences (Miller *et al.* 1996).

preignacite (Burns 1998c), agrinierite (Cahill & Burns 2000) and masuyite (Burns & Hanchar 1999), as well as a synthetic Cs uranyl oxide hydrate (Hill & Burns 1999). As such, it is apparent that sheets based upon this topology are compatible with a range of interlayer configurations involving Ba, Ca, Pb, K and Cs. This simple anion-topology contains only triangles and pentagons. Only **P** and **D** chains are required to develop the protasite anion-topology, with the repeat sequence **PDPD**…

Fourmarierite anion-topology

Sheets based upon the fourmarierite anion-topology (Fig. 5b) occur in fourmarierite (Piret 1985) and schoepite (Finch *et al.* 1996). In schoepite, the sheets are neutral, with H_2O groups being the only constituents of the interlayer. In fourmarierite, the sheets have a different distribution of O and $(OH)^-$, resulting in a charged sheet that is balanced by Pb^{2+} in the interlayer. The anion topology can be obtained with a chain-stacking sequence involving **P**, **D** and **U** chains, with the sequence **DUPUDPDU**…

Vandendriesscheite anion-topology

The vandendriesscheite anion-topology (Fig. 5c) is exceptionally complex, with a primitive repeat of 41.4 Å (Burns 1997). Only vandendriesscheite contains a sheet based upon this topology, which can be constructed using **P**, **U** and **D** chains in the sequence **PDUPUPUPU DPDPDPDUPUPUP**…. It contains sections that are identical to the **PDPD**… (or **PUPU**…) repeats of the protasite anion-topology, with the join between such sections involving the **DU** sequence of the fourmarierite anion-topology. Thus, the vandendriesscheite anion-topology is a structural intermediate between these two simpler anion-topologies.

Sayrite anion-topology

Sayrite (Piret *et al.* 1983) is the only mineral that contains sheets based upon the sayrite anion-topology, which involves **U**, **D**, **P**, and **R** chains (Fig. 5d). The chains are arranged such that each **P** chain is flanked by two arrowhead chains with the same sense (direction), giving **UPU** or **DPD** sequences. These two sequences alternate in the anion topology, and are separated by **R** chains, giving the sequence **RUPURDPDRUPU**…

Curite anion-topology

The structure of curite (Taylor *et al.* 1981) contains sheets based upon the curite anion-topology (Fig. 5e), which cannot be described as a simple chain-stacking sequence using only the **U**, **D**, **P** and **R** chains. A chain with pentagons, triangles and squares is required (Fig. 4b). It has a directional sense owing to the presence of an arrowhead (a pentagon and a triangle sharing an edge), and is designated $\mathbf{U^m}$ and $\mathbf{D^m}$, for up and down (modified) pointing chains, respectively. The curite anion-topology can be characterized by the chain-stacking sequence $\mathbf{U^mDU^mD}$… (Fig. 5e).

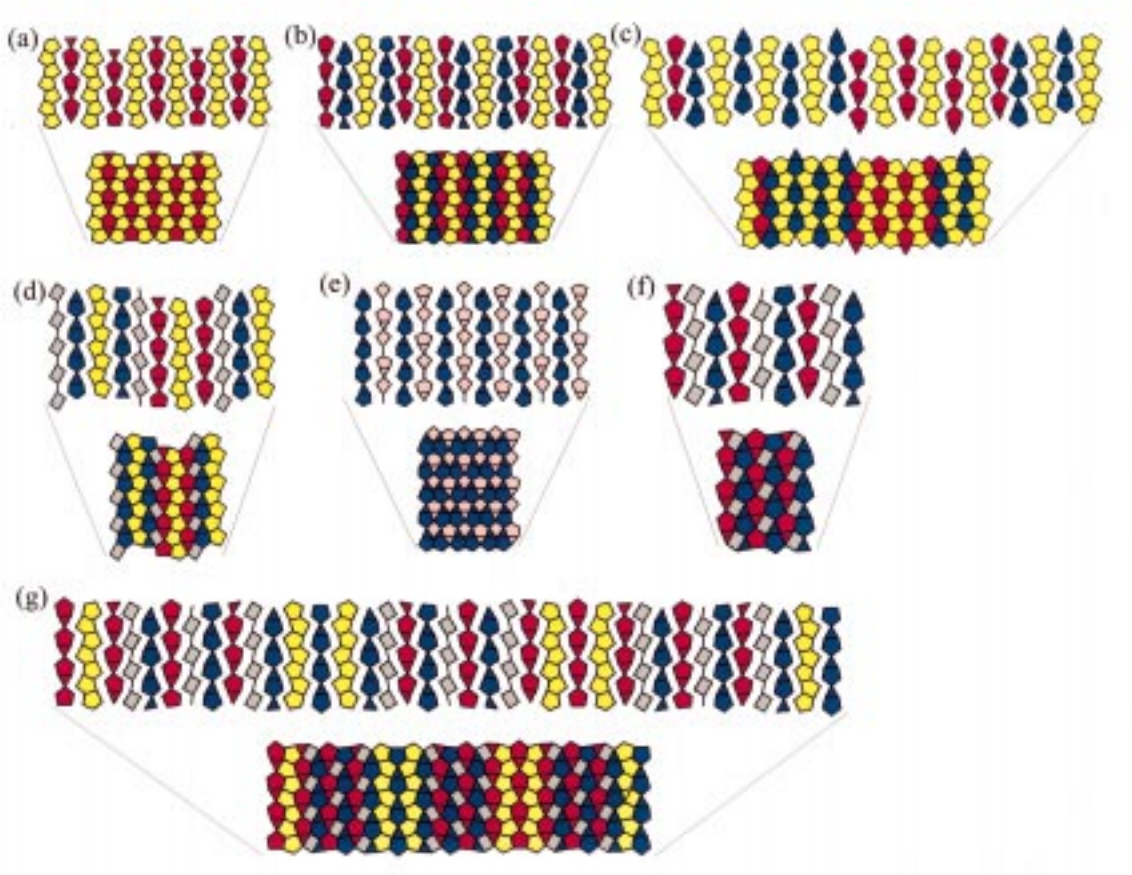

FIG. 5. Construction of anion topologies using chain-stacking sequences. (a) protasite anion-topology, (b) fourmarierite anion-topology, (c) vandendriesscheite anion-topology, (d) sayrite anion-topology, (e) curite anion-topology, (f) β–U_3O_8 anion-topology, (g) wölsendorfite anion-topology.

β–U_3O_8 anion-topology

The β–U_3O_8 sheet anion-topology (Fig. 5f) is the basis of the sheets in ianthinite (Burns *et al.* 1997a), as well as the sheets in β–U_3O_8. This topology can conveniently be described using a chain-stacking sequence involving **U**, **D** and **R** chains with the repeat sequence **DRUDRU**…

Wölsendorfite anion-topology

The sheet of uranyl polyhedra in the structure of wölsendorfite is based upon the anion-topology presented in Figure 5g. This anion topology is the most complex found to date, with a primitive repeat of 56 Å. It may be constructed using **R**, **D**, **P**, and **U** chains, with the repeat sequence **DRUDRUDRUPDPDRUDRU DRUPDP**… The repeat sequence involves the strings **DRUDRUDRU** and **PDP**, which are slabs of the β–U_3O_8 and protasite anion-topologies, respectively. Thus, the wölsendorfite anion-topology is structurally intermediate between the β–U_3O_8 and protasite anion-topologies.

Observations concerning chain-stacking sequences

Miller *et al.* (1996) used chain-stacking sequences to develop anion topologies that occur in uranyl oxide hydrates for which structures are known, and demonstrated that the approach could be used to predict new topologies. An interesting aspect of the chain-stacking sequences noted by Miller *et al.* (1996) is that **P** chains are always adjacent to either **U** or **D** chains in topologies, and the chains on either side of the **P** chain always have the same orientation, *i.e.*, both are either **U** or **D**. The wölsendorfite and vandendriesscheite anion-topologies, discovered since the work of Miller *et al.* (1996), exhibit the same relationship between **P**, **U** and **D** chains (Burns 1997, 1999a). Miller *et al.* (1996) noted that the degree of structural misfit is identical within the **UPU**,

DPD and **UPD** sequences; thus it is unclear why the **UPU** and **DPD** sequences dominate.

New anion topology in KUOH

The anion topology of *KUOH*, derived using the methods of Burns *et al.* (1996), is presented in Figure 6. The **U**, **D**, and **P** chains, as well as a distorted **R** chain, are required to construct the anion topology, which has not been previously reported. The chain stacking-sequence is **DUPDPUDRDUPDPUDR**… Although this anion topology contains chains found in other topologies, the arrangement of the chains is unique. Segments of alternating **UPDPU** and **DRD** occur in the chain-stacking sequence. The occurrence of the **UPDPU** sequence is remarkable, as it is the first occurrence of **P** chains flanked by **U** or **D** chains of opposite directional senses. This finding confirms the observation of Miller *et al.* (1996) that **P** chains need not be flanked by **U** or **D** chains of the same orientation. In addition, the occurrence of an **R** chain flanked by two **D** (or **U**) chains is unique to this topology.

Related Mineral Species

There are three K uranyl oxide hydrates that have been described as minerals: compreignacite, $K_2[(UO_2)_3O_2(OH)_3]_2(H_2O)_7$ (Protas 1964, Burns 1998c), agrinierite, $K_2(Ca,Sr)[(UO_2)_3O_3(OH)_2]\cdot 2.5H_2O$ (Cesbron *et al.* 1972, Cahill & Burns 2000), and rameauite, $K_2CaU_6O_{20}\cdot 9H_2O$ (Cesbron *et al.* 1972). Each of these have been reported from the Margnac deposit, Haute-Vienne, Massif Central, France, and formed following the alteration of uraninite in K-rich rocks. Elton *et al.* (1995) also reported the occurrence of compreignacite from Cornwall, England. On the basis of the chemical similarity of *KUOH* and the known K uranyl oxide hydrate minerals, nothing is apparent that precludes *KUOH* from occurring as a mineral in a similar geological environment.

Conclusion

The new topology found in *KUOH* again demonstrates the amazing complexity possible in sheets of uranyl polyhedra, and supports the hypothesis that many more sheets may exist. It is conceivable that many of these sheets are energetically similar, thus their occurrences may be sensitive indicators of geochemical conditions at the time of crystal growth.

Acknowledgements

This research was funded by the Environmental Management Sciences Program of the United States Department of Energy (DE–FG07–97ER14820). The

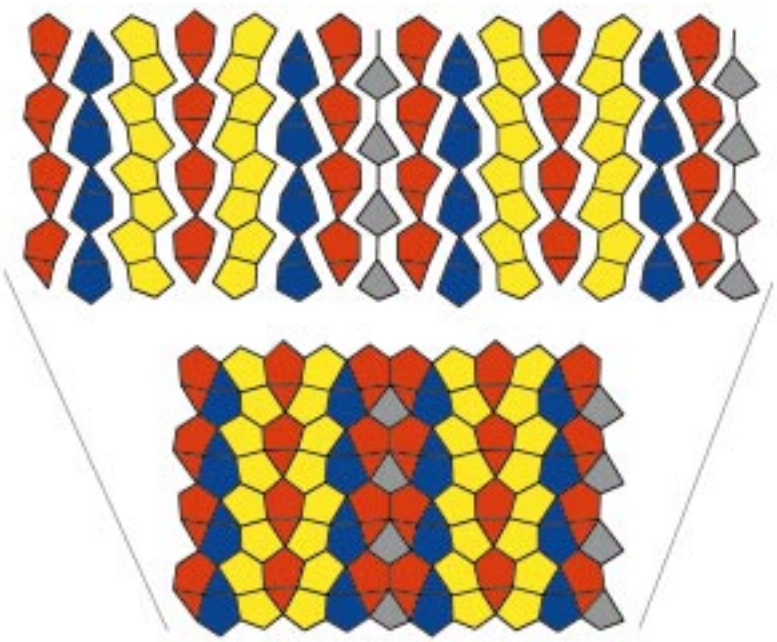

FIG. 6. Construction of the *KUOH* sheet anion-topology using a chain-stacking sequence.

manuscript was improved following reviews provided by two anonymous referees, and editorial work by R.F. Martin.

REFERENCES

BRESE, N.E. & O'KEEFFE, M. (1991): Bond-valence parameters for solids. *Acta Crystallogr.* **B47**, 192-197.

BURNS, P.C. (1997): A new uranyl oxide hydrate sheet in the structure of vandendriesscheite: implications for mineral paragenesis and the corrosion of spent nuclear fuel. *Am. Mineral.* **82**, 1176- 1186.

_____ (1998a): CCD area detectors of X-rays applied to the analysis of mineral structures. *Can. Mineral.* **36**, 847-853.

_____ (1998b): The structure of richetite, a rare lead uranyl oxide hydrate. *Can. Mineral.* **36**, 187-199.

_____ (1998c): The structure of compreignacite, $K_2[(UO_2)_3O_2(OH)_3]_2(H_2O)_7$. *Can. Mineral.* **36**, 1061-1067.

_____ (1998d): The structure of boltwoodite and implications of solid solution toward sodium boltwoodite. *Can. Mineral.* **36**, 1069-1075.

_____ (1999a): A new complex sheet of uranyl polyhedra in the structure of wölsendorfite. *Am. Mineral.* **84**, 1661-1673.

_____ (1999b): The crystal chemistry of uranium. *In* Uranium: Mineralogy, Geochemistry and the Environment (P.C. Burns & R. Finch, eds.). *Rev. Mineral.* **38**, 23-90.

_____ (2000a): A new uranyl silicate sheet in the structure of haiweeite and comparison to other uranyl silicates. *Can. Mineral.* **38** (in press).

_____ (2000b): A new uranyl phosphate chain in the structure of parsonsite. *Am. Mineral.* **85** (in press).

_____, EWING, R.C. & HAWTHORNE, F.C. (1997b): The crystal chemistry of hexavalent uranium: polyhedral geometries, bond-valence parameters, and polyhedral polymerization. *Can. Mineral.* **35**, 1551-1570.

_____ & FINCH, R.J. (1999): Wyartite: crystallographic evidence for the first pentavalent-uranium mineral. *Am. Mineral.* **84**, 1456-1460.

_____, _____, HAWTHORNE, F.C., MILLER, M.L. & EWING, R.C. (1997a): The crystal structure of ianthinite, $[U^{4+}{}_2(UO_2)_4O_6(OH)_4(H_2O)_4](H_2O)_5$: a possible phase for Pu^{4+} incorporation during the oxidation of spent nuclear fuel. *J. Nucl. Mater.* **249**, 199-206.

_____ & HANCHAR, J.M. (1999): The structure of masuyite, $Pb[(UO_2)_3O_3(OH)_2](H_2O)_3$, and its relationship to protasite. *Can. Mineral.* **37**, 1483-1491.

_____ & HILL, F.C. (2000): Implications of the synthesis and structure of the Sr analogue of curite. *Can. Mineral.* **38** (in press).

_____, MILLER, M.L. & EWING, R.C. (1996): U^{6+} minerals and inorganic phases: a comparison and hierarchy of crystal structures. *Can. Mineral.* **34**, 845-880.

CAHILL, C.L. & BURNS, P.C. (2000): The structure of agrinierite: a Sr-containing uranyl oxide hydrate mineral. *Am. Mineral.* **85** (in press).

CESBRON, F., BROWN, W.L., BARIAND, P. & GEFFROY, J. (1972): Rameauite and agrinierite, two new hydrated uranyl oxides from Margnac, France. *Mineral. Mag.* **38**, 781-789.

ELTON, N.J., HOOPER, J.J. & RYBACK, G. (1994): Compreignacite: a second occurrence, from St. Just, Cornwall. *Mineral. Mag.* **58**, 339-341.

EVANS, H.T., JR. (1963): Uranyl ion coordination. *Science* **141**, 154-157.

FINCH, R.J., COOPER, M.A. & HAWTHORNE, F.C. (1996): The crystal structure of schoepite, $[(UO_2)_8O_2(OH)_{12}](H_2O)_{12}$. *Can. Mineral.* **34**, 1071-1088.

_____ & EWING, R.C. (1992): The corrosion of uraninite under oxidizing conditions. *J. Nucl. Mater.* **190**, 133-156.

FINN, P.A., HOH, J.C., WOLF, S.F., SLATER, S.A. & BATES, J.K. (1996): The release of uranium, plutonium, cesium, strontium, technetium and iodine from spent fuel under unsaturated conditions. *Radiochim. Acta* **74**, 65-71.

FRONDEL, C. (1958): Systematic mineralogy of uranium and thorium. *U.S. Geol. Surv., Bull.* **1064**.

HILL, F.C. & BURNS, P.C. (1999): The structure of a synthetic Cs uranyl oxide hydrate and its relationship to compreignacite. *Can. Mineral.* **37**, 1283-1288.

IBERS, J.A. & HAMILTON, W.C., eds. (1974): *International Tables for X-ray Crystallography* **IV**. The Kynoch Press, Birmingham, U.K.

MANDARINO, J.A. (1999): *Fleischer's Glossary of Mineral Species 1999*. The Mineralogical Record Inc., Tucson, Arizona.

MILLER, M.L., FINCH, R.J., BURNS, P.C. & EWING, R.C. (1996): Description and classification of uranium oxide hydrate sheet topologies. *J. Mater. Res.* **11**, 3048-3056.

PAGOAGA, M.K., APPLEMAN, D.E. & STEWART, J.M. (1987): Crystal structures and crystal chemistry of the uranyl oxide hydrates becquerelite, billietite, and protasite. *Am. Mineral.* **72**, 1230-1238.

PIRET, P. (1985): Structure cristalline de la fourmariérite, $Pb(UO_2)_4O_3(OH)_4{\cdot}4H_2O$. *Bull. Minéral.* **108**, 659-665.

_____, DELIENS, M., PIRET-MEUNIER, J. & GERMAIN, G. (1983): La sayrite, $Pb_2[(UO_2)_5O_6(OH)_2]{\cdot}4H_2O$, nouveau minéral; propriétés et structure cristalline. *Bull. Minéral.* **106**, 299-304.

PROTAS, J. (1964): Une nouvelle espèce minérale: la compreignacite, $K_2O•6UO_3•11H_2O$. *Bull. Soc. Fr. Minéral. Cristallogr.* **87**, 365-371.

TAYLOR, J.C., STUART, W.L. & MUMME, I.A. (1981) The crystal structure of curite. *J. Inorg. Nucl. Chem.* **43**, 2419-2423.

VOCHTEN, R., BLATON, N., PEETERS, O., VAN SPRINGEL, K. & VAN HAVERBEKE, L. (1997): A new method of synthesis of boltwoodite and of formation of sodium boltwoodite, uranophane, sklodowskite and kasolite from boltwoodite. *Can. Mineral.* **35**, 735-741.

WRONKIEWICZ, D.J., BATES, J.K., WOLF, S.F. & BUCK, E.C. (1996): Ten-year results from unsaturated drip tests with UO_2 at 90°C: implications for the corrosion of spent nuclear fuel. *J. Nucl. Mater.* **238**, 78-95.

Received May 26, 1999, revised manuscript accepted December 15, 1999.